HHS Public Access

Author manuscript

J Physiol. Author manuscript; available in PMC 2021 July 01.

Published in final edited form as:

J Physiol. 2020 July ; 598(13): 2651–2667. doi:10.1113/JP279658.

Intracellular acidification facilitates receptor-operated TRPC4 activation through PLCδ1 in a Ca^{2+}-dependent manner

Dhananjay P. Thakur[*,†], **Qiaochu Wang**[†], **Jaepyo Jeon**, **Jin-Bin Tian**, **Michael X. Zhu**

Department of Integrative Biology and Pharmacology, McGovern Medical School, The University of Texas Health Science Center at Houston, Houston, TX 77030, USA

Abstract

Transient Receptor Potential Canonical 4 (TRPC4) forms non-selective cation channels activated downstream from receptors that signal through G proteins. Our recent work suggests that TRPC4 channels are particularly coupled to pertussis toxin-sensitive $G_{i/o}$ proteins, with a co-dependence on phospholipase-Cδ1 (PLCδ1). The $G_{i/o}$-mediated TRPC4 activation is dually dependent on and bimodally regulated by phosphatidylinositol 4,5-bisphosphate (PIP_2), the substrate hydrolysed by PLC, and intracellular Ca^{2+}. As a byproduct of PLC-mediated PIP_2 hydrolysis, protons have been shown to play an important role in the activation of *Drosophila* TRP channels. However, how intracellular pH affects mammalian TRPC channels remains obscure. Here, using patch-clamp recordings of HEK293 cells heterologously co-expressing mouse TRPC4β and the $G_{i/o}$-coupled μ opioid receptor, we investigated the role of intracellular protons on $G_{i/o}$-mediated TRPC4 activation. We found that acidic cytosolic pH greatly accelerated the rate of TRPC4 activation without altering the maximal current density and this effect was dependent on intracellular Ca^{2+} elevation. However, protons did not accelerate channel activation by directly acting upon TRPC4. We additionally demonstrated that protons exert their effect through sensitization of PLCδ1 to Ca^{2+}, which in turn promotes PLCδ1 activity and further potentiates TRPC4 via a positive feedback mechanism. The mechanism elucidated here helps explain how $G_{i/o}$ and $G_{q/11}$ co-stimulation induces a faster activation of TRPC4 than $G_{i/o}$ activation alone and highlights again the critical role of PLCδ1 in TRPC4 gating.

Corresponding author M. X. Zhu: Department of Integrative Biology and Pharmacology, the University of Texas Health Science Centre at Houston, MSB 4.128, 6431 Fannin St., Houston, TX 77030, USA. Michael.X.Zhu@uth.tmc.edu.

[*]Current address: Neuroscience Research Institute, University of California, Santa Barbara, CA, USA

[†]These authors contributed equally.

Author contributions

D.P.T., Q.W. and M.X.Z. conceptualized the research and designed the experiments. D.P.T., Q.W., J.J. and J.B.T. performed experiments and analysed the data. D.P.T., Q.W. and M.X.Z. wrote the manuscript. All authors have read and approved the final version of the manuscript, and agree to be accountable for all aspects of the work in ensuring that questions related to the accuracy or integrity of any part of the work are appropriately investigated and resolved. All persons designated as authors qualify for authorship, and all those who qualify for authorship are listed.

Competing interests

The authors declare no conflicts of interest.

Data availability

The data that support the findings of this study are available from the corresponding author upon reasonable request.

Supporting information

Additional supporting information may be found online in the Supporting Information section at the end of the article.

Keywords

calcium; Gi/o proteins; PLCδ1; protons; PTX; TRP channels

Introduction

Transient receptor potential (TRP) channels function as sensors of a wide variety of stimuli from both intracellular and extracellular environments (Clapham, 2003). They also act as integrators of signal transduction via gating cations and initiating further intracellular signalling cascades (Venkatachalam & Montell, 2007). Within the TRP channel superfamily, canonical TRP (TRPC) channels have been implicated in the regulation of many physiological functions including vascular tone, endothelial permeability, gastrointestinal contractility and motility, neurite growth, neurotransmitter release, excitotoxicity, and neurodegeneration (Tian *et al.* 2014*a*). It is believed that membrane depolarization and intracellular Ca^{2+} elevation resulting from TRPC channel activation are responsible for these functions (Venkatachalam & Montell, 2007; Tian *et al.* 2014*a*).

TRPC channels are generally thought to be activated through pathways that couple to stimulation of phospholipase C (PLC), which typically occur downstream of certain G protein-coupled receptors (GPCRs) or receptor tyrosine kinases (RTKs). PLC hydrolyses phosphatidylinositol 4,5-bisphosphate (PIP_2) to yield inositol 1, 4, 5-trisphosphate (IP_3), diacylglycerol (DAG) and protons (H^+). Interestingly, both the substrate and the products of PLC have been implicated in TRPC channel regulation. PIP_2 exerts both inhibitory and facilitatory effects on TRPCs (Lemonnier *et al.* 2008; Otsuguro *et al.* 2008; Trebak *et al.* 2009; Kim *et al.* 2013). DAG can directly activate these channels (Hofmann *et al.* 1999; Storch *et al.* 2017). IP_3 may activate some TRPC channels by stimulating IP_3 receptors which bind directly to the TRPC channels (Kiselyov *et al.* 1998; Zhang *et al.* 2001) and/or by causing an increase in intracellular Ca^{2+} concentration ($[Ca^{2+}]_i$) through mobilizing Ca^{2+} from the endoplasmic reticulum (ER) stores (Shi *et al.* 2004; Blair *et al.* 2009; Thakur *et al.* 2016). Even H^+, the often neglected byproduct of PIP_2 hydrolysis, has been shown to support the activation of *Drosophila* TRPCs, TRP and TRPL, in insect photoreceptors, together with phosphoinositide depletion or changes in membrane mechanical properties (Huang *et al.* 2010; Randall *et al.* 2015). However, how intracellular protons affect mammalian TRPC channels remains obscure.

In the current study, we examined the effect of intracellular protons on the activation of mouse TRPC4 by stimulation of $G_{i/o}$-coupled μopioid receptors (μORs). TRPC4 is unique among the TRPC channels in that its activation requires not only PLC but also pertussis toxin (PTX)-sensitive $G_{i/o}$ proteins (Jeon *et al.* 2012, 2016; Thakur *et al.* 2016). For $G_{i/o}$ proteins, it was shown that the GTP-bound $G\alpha_{i2}$, $G\alpha_{i3}$ and $G\alpha_o$ subunits, but not $G\alpha_{i1}$ or $G\beta\gamma$, might be responsible for TRPC4 activation (Jeon *et al.* 2012). For PLC, the PLCδ1 isoform appears to be essential for receptor-operated TRPC4 channel activation, as specific inhibition of PLCδ1 with either a dominant-negative PLCδ1 mutant (DN-PLCδ1) or a constitutively active form of RhoA (CA-RhoA), a small GTPase known to suppress PLCδ1 activity through direct physical interactions (Hodson *et al.* 1998), completely abolished

TRPC4 activation irrespective of other PLC iso-forms activated via $G_{q/11}$ or RTK (Thakur *et al.* 2016). However, in the absence of stimulation of $G_{q/11}$-PLCβ or RTK-PLCγ, PLCδ1 is rate-limiting and is probably responsible for the biphasic development of $G_{i/o}$-mediated TRPC4 activation (Thakur *et al.* 2016). As the prototypical PLC isozyme, PLCδ1 is solely activated by Ca^{2+}, being the most sensitive to Ca^{2+} among all PLC isozymes (Rhee & Bae, 1997; Murthy *et al.* 2004). However, increasing $[Ca^{2+}]_i$ by a Ca^{2+} ionophore, ionomycin (IM), only enhanced the probability, but not the rate, of $G_{i/o}$-mediated TRPC4 activation (Thakur *et al.* 2016), ruling out global $[Ca^{2+}]_i$ rise as the main rate-limiting factor. Here, we show that the $G_{i/o}$-mediated TRPC4 activation is accelerated by a decrease in intracellular pH (pH_i). This effect is dependent on elevated $[Ca^{2+}]_i$ and exerted through PLCδ1.

Methods

Reagents and cDNA

(D-Ala2, N-MePhe4, Gly-ol)-enkephalin (DAMGO) was bought from Bachem Chemicals Co. (Torrance, CA, USA); carbamylcholine (carbachol) and IM were from Sigma-Aldrich (St Louis, MO, USA). Englerin A was from Cerilliant Corp (Round Rock, TX, USA). cDNAs for mouse TRPC4β, TRPC4α and TRPC5 were cloned in the pIRES-neo vector. The E542Q/E543Q mutant of TRPC4β was generated using a QuikChange site-directed mutagenesis kit (Agilent Technologies, Santa Clara, CA, USA) following the manufacturer's protocol. The sequence was verified by DNA sequencing. The cDNA for μOR was cloned in pIRES-hygro vectors. The cDNA construct for DrVSP was kindly provided by Dr Y. Okamura (Okazaki Institute for Integrative Bioscience) and was subcloned into a pIRES2-EGFP vector. The cDNA for human PLCδ1 was obtained from the Dana-Farber/Harvard Cancer Center DNA Resource Core (Harvard University, Cambridge, MA, USA). The dominant negative PLCδ1 mutant (DN-PLCδ1, E341R/D343R in pCMV-SPORT6) was created as described (Thakur *et al.* 2016). TagRFP-DN-PLCδ1 was created by subcloning the coding sequence of DN-PLCδ1 to pTagRFP-C vector (Evrogen, Moscow, Russia). cDNAs for RhoA and RhoA mutants (CA and N19) and C3 exoenzyme were kindly provided by Dr J. Frost (University of Texas Health Science Center at Houston). KCNQ2 and KCNQ3-CFP plasmids were kindly provided by Dr Mark Shapiro (University of Texas Health Science Center at San Antonio).

Cell culture

HEK293 cells were grown in Dulbecco's modified Eagle's medium (DMEM) containing 10% (v/v) fetal bovine serum (FBS), 2 mM L-glutamine at 37°C in a humidity-controlled incubator with 5% CO_2. Stable HEK293 cell lines expressing μOR alone and μOR plus TRPC4β, TRPC4α or TRPC5 were created and maintained as described previously (Otsuguro *et al.* 2008; Miller *et al.* 2011). All cell culture reagents were purchased from Invitrogen (Carlsbad, CA, USA). For transient transfection, cells were seeded in wells of a 12-well plate and allowed to grow overnight. The following day, transfection was carried out using polyethylenimine (PEI) and a total of 0.5 μg per well cDNA. Electrophysiological recordings were performed between 24 and 48 h after transfection. Cells were seeded on 12- or 15-mm coverslips coated with poly-L-ornithine between 4 and 16 h before patch clamp recordings or imaging.

Electrophysiological recording of TRPC currents

Transiently transfected cells were identified by enhanced green fluorescent protein (EGFP) encoded in the plasmid for the protein of interest or the co-transfected pEGFP-N1 vector. Recording pipettes were pulled from micropipette glass (Sutter Instruments, Novato, CA, USA) to 3–5 MΩ when filled with a pipette solution containing (in mM): 140 CsCl, 1 $MgCl_2$, EGTA and 10 Hepes; pH and EGTA concentrations in the pipette solutions were varied as indicated in the figure legends. For pipette solutions with 50 and 100 mM Hepes, CsCl was reduced to 120 and 95 mM, respectively, to maintain osmolarity. After adjusting the pH with CsOH, the final caesium concentrations of these solutions ranged from 148 to 153 mM. Bath solutions (pH 7.4) contained (in mM): 140 NaCl, 5 KCl, 2 $CaCl_2$, 1 $MgCl_2$, 10 glucose and 10 Hepes, except where indicated otherwise. Isolated cells were voltage-clamped in the whole-cell mode using an Axon 200B amplifier and 1440A Digitizer (Molecular Devices, Sunnyvale, CA, USA) or an EPC10 (HEKA Instruments, Bellmore, NY, USA) amplifier. Currents were recorded at 2 kHz. Voltage commands (explained in the figure legends) were made from either pCLAMP 10 (Molecular Devices) or PatchMaster (version 2×90.1; HEKA) software. For whole-cell recordings, a membrane test pulse was applied every 10 s to test for membrane resealing. Cells that resealed were eliminated from analysis. Drugs were diluted to the final concentration in the bath solutions and applied to the cell through perfusion. Cells were continuously perfused with the bath solution through a gravity-driven multi-outlet device with the desired outlet placed ~50 μm away from the cell being recorded except in the case of Englerin-A, for which the perfusion outlet was placed outside the bath solution and introduced into the solution ~50 μm away from the cell 5–15 s before addition of the drug.

Calibration of pH_i changes induced by sodium acetate (NaAc) gradients

Cells stably expressing TRPC4β and μOR were voltage-clamped at −60 mV with a pipette solution (pH 7.4) that contained (in mM): 140 CsCl, 5 NaAc, 1 $MgCl_2$, 0.05 EGTA and 10 Hepes, supplemented with 300 μM BCECF (2′,7′-bis-(2-carboxyethyl)-5-(and-6)-carboxyfluorescein; free K^+ salt). The initial bath solution (pH 7.4) contained (in mM): 140 NaCl, 5 KCl, 2 $CaCl_2$, 1 $MgCl_2$, 10 glucose and 10 Hepes. After establishment of the whole-cell configuration and dialysis for >5 min, the bath was changed to a solution in which an equal molar NaCl was replaced with 7.9, 39.5 or 125.4 mM NaAc (all at pH 7.4) with the expected intracellular pH drop to 7.2, 6.5 or 6.0, while BCECF fluorescence images were taken at alternating excitations of 440 and 490 nm, and emission at 535 nm, with 3 s intervals. At the end of the experiment, the cells were exposed to calibration solutions containing (in mM) 145 KCl, 2 $CaCl_2$, 1 $MgCl_2$, 10 glucose, 10 Hepes and 10 μM nigericin, with pH adjusted to 7.2, 6.5 and 6.0, and BCECF fluorescence images continuously taken. pH values for individual cells (regions of interest) were determined from the calculated ratios of BCECF emission intensities produced by the excitation at ~490 nm to that at its isobestic point of ~440 nm after background subtraction. Background subtracted $F_{490/440}$ ratios from KCl/nigericin calibration (means ± SD, $n = 5$ for each pH) were used to generate the standard curve by linear regression fit. For changing intracellular pH without an alteration in extracellular pH during the whole-cell experiments, the same pipette and bath solutions as described in this section, except for the omission of BCECF, were used.

Assessing PLC activity through whole-cell recording of KCNQ2/3 current

Cells stably expressing μOR were transiently transfected with KCNQ2 and KCNQ3-CFP plasmids at a 1:1 ratio and used for experiments within 24 h. When needed, the cDNA for TagRFP-DN-PLCδ1 was included at a ratio of 1:1:1 (KCNQ2/KCNQ3/TagRFP-DN-PLCδ1), and that for CA-RhoA at a ratio of 1:1:3 (KCNQ2/KCNQ3/CA-RhoA). Recordings were performed with an EPC10 (HEKA Instruments) amplifier and voltage commands were made from the PatchMaster program (version 2×90.1; HEKA). The pipette solution (pH 7.4) contained (in mM): 140 KCl, 5 NaAc, 1 $MgCl_2$, 0.05 EGTA, 10 Hepes and 3 ATP. The bath solution contained (in mM): 140 NaCl, 5 KCl, 2 $CaCl_2$, 1 $MgCl_2$, 10 glucose and 10 Hepes, pH 7.4. Cells were held at −60 mV and 600-ms steps to 0 mV were applied every 2.5 s to repetitively elicit a KCNQ2/3 current. Currents were recorded at 2.9 kHz and filtered at 1.0 kHz. For switching pH_i to 7.2 and 6.5, the bath was changed to solutions in which an equal molar NaCl was replaced with 7.9 and 39.5 mM NaAc (all at pH 7.4), respectively. This was followed by the addition of IM (1 μM) in the same solution to evoke PLC activation. Steady-state currents were used to assess the decay of KCNQ2/3 currents, which reflected the decrease of PIP_2 content due to increased PLC activity.

Data presentation and statistical analysis

All summary data are expressed as means ± SD. Statistical significance was determined using Student's *t* tests or one-way ANOVA with Tukey's multiple comparisons test. $P < 0.05$ were considered statistically significant. Graphs were generated by Graphpad Prism 5 (Version 5.01).

Results

Protons cooperate with $[Ca^{2+}]_i$ rise to facilitate $G_{i/o}$-mediated activation of TRPC4β

Previously, using an HEK293 stable cell line co-expressing TRPC4β and μOR, we determined that the full activation of TRPC4β required both $G_{i/o}$ and PLCδ1, which are endogenously present in the cells (Thakur *et al.* 2016). Although μOR stimulation alone was sufficient for TRPC4β activation, the kinetics was very slow. As shown in Fig. 1*A*, the μOR agonist DAMGO (1 μM) evoked TRPC4β currents with biphasic kinetics. However, co-application of DAMGO (1 μM) with carbachol (CCh, 30 μM), an agonist of endogenously expressed muscarinic receptors that activates PLCβ through $G_{q/11}$, resulted in rapid current development with monophasic kinetics (Fig. 1*B*). The time required to reach 90% of the peak current (T_{90}) was significantly shortened by ~15 s (Fig. 1*G*). Thus, certain constituents of the $G_{q/11}$-PLCβ signaling must be important for accelerating $G_{i/o}$-dependent TRPC4 activation.

We showed previously that increasing $[Ca^{2+}]_i$ by IM enhanced the probability, but not kinetics, of DAMGO-induced TRPC4β activation (Thakur *et al.* 2016). This slow kinetics is also shown here (Fig. 1*C*). Thus, $[Ca^{2+}]_i$ elevation is not the key factor associated with $G_{q/11}$-PLCβ signalling that accelerates TRPC4 activation. In our previous study, we also ruled out the contribution of DAG, IP_3 or protein kinase C (PKC) in the activation kinetics of TRPC4 (Thakur *et al.* 2016). Therefore, we turned our attention to protons. Comparing cells bathed in the pH 7.4 and pH 6.8 extracellular solutions, the moderately acidic

extracellular pH (pH_e) of 6.8 significantly accelerated DAMGO-induced TRPC4β activation in the presence of IM, with a comparable average T_{90} as that triggered by the co-application of DAMGO and CCh (Fig. 1*D* and G). The facilitation by low pH_e was also detected in the absence of IM, but to a lower degree (Fig. 1*G*). Notably, without DAMGO, IM did not elicit any detectable TRPC4β current, even in the acidic solution (Fig. 1*C* and D), suggesting that the facilitatory effect of protons on TRPC4β activation depends exclusively on $G_{i/o}$ stimulation.

A potentiation effect of extracellular protons on TRPC4 and TRPC5 activation has been reported before and, at least for TRPC5, it was attributed to an acidic residue, Glu543, in the pore loop (Semtner *et al.* 2007). The equivalent residues, Glu542 and Glu543, on TRPC4β could also be responsible for the low pH_e-induced acceleration of TRPC4β activation. To test this possibility, we neutralized the two glutamates to glutamines and expressed the resulting mutant, E542Q/E543Q, transiently in μOR-expressing HEK293 cells. However, at neutral pH_e, the mutant still exhibited biphasic activation kinetics in response to DAMGO, even in the presence of IM (Fig. 1*E*). With the pH_e lowered to 6.8, the activation of TRPC4β (E542Q/E543Q) became faster and almost monophasic (Fig. 1*F*), with the mean T_{90} value approaching that evoked by the co-stimulation with CCh and DAMGO (Fig. 1*G*). Importantly, the low pH_e only affected the activation kinetics (Fig. 1*G*), but not the peak current density evoked by DAMGO (Fig. 1*H*). These results demonstrate that protons uniquely regulate the kinetics of $G_{i/o}$-dependent TRPC4 activation and the effect is not entirely mediated by the known extracellular protonation residues in the pore loop.

Increased intracellular [H^+] accelerates kinetics of $G_{i/o}$ activation of TRPC4β

It is well known that extracellular acidification also causes a decrease in pH_i (Salvi *et al.* 2002; Wang *et al.* 2015; Gao *et al.* 2016). To directly test the effect of lowering pH_i on $G_{i/o}$-mediated TRPC4β activation, we first used a pH 6.5 pipette solution buffered with 50 mM Hepes. The high Hepes concentration was intended to minimize pH_i fluctuations during the recording. In the presence of IM, pH_i 6.5 allowed DAMGO to elicit a monophasic current, with a mean T_{90} of <8 s (Fig. 2*A* and E). By contrast, without IM, pH_i 6.5 did not abolish the biphasic response and the mean T_{90} was >12 s (Fig. 2*B* and E). Although the difference between pH_i 6.5 in the presence and absence of IM ($p = 0.066$) and that between pH_i 7.2 and pH_i 6.5 in the presence of IM ($p = 0.060$) did not reach statistical significance under these experimental conditions (Fig. 2*E*), the trend for low pH_i to shorten T_{90} in the presence of IM provided the first evidence that intracellular protons might regulate the rate of $G_{i/o}$-mediated TRPC4β activation in a $[Ca^{2+}]_i$-dependent manner.

PLC activation causes PIP_2 breakdown to generate DAG, IP_3 and protons near the plasma membrane. We reasoned that the local production of protons generated from the breakdown of PIP_2 after $G_{q/11}$-PLCβ activation might underlie the accelerating effect of CCh on DAMGO-evoked TRPC4 activation. In line with this prediction, when the pipette solution was maintained at an alkalized pH_i of 8.5 buffered by 100 mM Hepes, the co-application of DAMGO and CCh evoked a slowly developing current with biphasic kinetics (Fig. 2*D* and E). However, this was not the case if the pH buffer was weakened by using 10 mM Hepes (Fig. 2*C* and E), indicating that the local proton generation contributed to the acceleration of

TRPC4β activation by $G_{q/11}$-PLCβ signalling. Furthermore, the pH_i 8.5 pipette solution reversed the accelerating effects of extracellular acidification (pH_e 6.8) on both wild-type (WT) TRPC4β and E542Q/E543Q (Fig. 2*G*–I), supporting the idea that the extracellularly applied protons exerted their effect on accelerating TRPC4β activation through intracellular acidification. Notably, all these treatments resulted in similar maximal current densities (Fig. 2*F* and J), supporting again the idea that protons mainly regulate the kinetics of TRPC4 activation.

Dual effects of intracellular protons on accelerating TRPC4 activation

Low pH pipette solutions might elicit non-specific effects that interfere with the kinetic measurement of $G_{i/o}$-mediated TRPC4 currents. Additionally, it was difficult to change pH_i at the desired time points without an efficient intracellular solution exchange system. To circumvent these limitations, we utilized the NaAc gradient method (Yuan *et al.* 2003; Niemeyer *et al.* 2010), which allows pH_i to be changed through bath perfusion while maintaining a constant pH_e of 7.4. Briefly, a whole-cell configuration was established with 5mM NaAc included in the pipette solution at pH 7.4. The desired pH_i, 7.2, 6.5, 6.25 and 6.0, could then be obtained by increasing extracellular NaAc concentrations to 7.9, 39.5, 71 and 125.4 mM, respectively. Using the pH indicator, BCECF, dialysed into cells under the same conditions as for the whole-cell recording, we confirmed these predicted pH_i changes by fluorescence ratio measurements (Fig. 3*A*).

Using the NaAc gradients to manipulate pH_i, we examined the kinetics and maximal current density of $G_{i/o}$-mediated TRPC4β activation in the presence and absence of IM. Although changing pH_i from 7.4 to different values ranging from 7.2 to 6.0 at the same time when IM was added did not elicit any currents, the sub-sequent application of DAMGO evoked TRPC4β currents, with varying kinetic patterns. We found that in the presence of IM, pH_i ranging from 6.75 to 6.25 abolished the biphasic current development and markedly decreased T_{90} of the DAMGO-evoked TRPC4β current by >10 s as compared to pH_i 7.2 (Fig. 3*Ba*–Bc and E). However, the biphasic pattern appeared again and T_{90} became even longer when pH_i was lowered to 6.0 (Fig. 3*Bd* and E). This indicates that the pH regulation of $G_{i/o}$-dependent TRPC4 activation is bidirectional. After fitting the data with a biphasic Hill equation (Foskett *et al.* 2007), we determined that the half maximal facilitation pH_i was 7.25 and the half maximal inhibition pH_i was 6.09. Remarkably, in the absence of IM, T_{90} remained relatively constant across the entire pH_i range tested, indicating that the facilitatory and inhibitory effects of protons are both dependent on $[Ca^{2+}]_i$ (Fig. 3*E*). Different from the kinetics, the peak current densities of DAMGO-evoked TRPC4 currents showed similar biphasic trends in response to the pH_i change in the presence and absence of IM, albeit not reaching statistical significance (Fig. 3*F*).

TRPC4β lacks 84 amino acids at the cytoplasmic C-terminus that are present in the TRPC4α isoform. Additionally, TRPC4 and TRPC5 share a similar gating mechanism and they can also form hetero oligomers (Plant & Schaefer, 2003). Therefore, we investigated whether the observed dual effect of pH_i regulation on TRPC4β is common for TRPC4α and TRPC5. Using stable cell lines that co-expressed μOR with either TRPC4α or TRPC5, we found that TRPC4α is under a similar bi-directional regulation by pH_i to TRPC4β (Fig. 3*C*

and E). However, TRPC5 was only facilitated, but not inhibited by protons, at least in the range from pH_i 7.2 to pH_i 6.0 (Fig. 3*Da*–Dc and E). Again similar to TRPC4β, the effects of pH_i on TRPC4α and TRPC5 were only detected in the presence of IM, implicating a dependence on $[Ca^{2+}]_i$ rise. These data demonstrate a common mechanism that moderate intracellular acidification (pH_i 6.75–6.25) facilitates $[Ca^{2+}]_i$-dependent $G_{i/o}$-mediated activation of TRPC4 and TRPC5 channels.

Intracellular protons inhibit TRPC4 activation by its direct agonist

$G_{i/o}$-coupled TRPC4 activation is exclusively dependent on PLCδ1 (Thakur *et al.* 2016). The facilitatory effect of intracellular protons could reflect an intrinsic property of the TRPC4 channel itself, the property of PLCδ1 or that of the μOR-mediated $G_{i/o}$ protein activation. To distinguish these possibilities, we first tested the effect of intracellular acidification on Englerin A-evoked TRPC4β currents.

Englerin A is a specific TRPC4/C5 agonist that evokes TRPC4 activation bypassing intracellular signalling pathways (Akbulut *et al.* 2015). Consistent with this idea, the Englerin A-evoked TRPC4 current was unaffected by depleting PIP_2 using the zebrafish voltage-sensitive phosphatase (DrVSP) (Fig. 4*A*–D). When co-expressed with ion channels, the activation of DrVSP in response to a strong depolarization pulse caused PIP_2 dephosphorylation to PIP without concomitantly generating the common PIP_2 hydrolysis products. Previously, we showed that DrVSP treatment led to a ~30–40% inhibition of the DAMGO-evoked TRPC4β currents at −60 mV, indicating a dependence on PIP_2 (Thakur *et al.* 2016). Here, activating DrVSP through depolarization pulses affected neither the maximal TRPC4β current density evoked by Englerin A (Fig. 4*C*) nor the sustaining of such current immediately following the voltage pulse (Fig. 4*D*). The complete insensitivity to DrVSP activation, thus, demonstrates that unlike the $G_{i/o}$-mediated response, the activation of TRPC4β by Englerin A is independent of PIP_2. This may be taken as a lack of dependence on PLCδ1, as the membrane targeting and function of PLCδ1 require PIP_2 (Garcia *et al.* 1995; Lomasney *et al.* 1996).

On the other hand, the Englerin A-evoked activation of TRPC4β exhibited a strong dependence on $[Ca^{2+}]_i$. Englerin A only activated TRPC4 when intracellular Ca^{2+} was weakly buffered by 0.05 mM EGTA, but not when 5 mM EGTA was included in the pipette solution (Fig. 4*E* and F). Using pipette solutions with $[Ca^{2+}]_i$ clamped to different levels (0.010–3 μM) by 5 mM BAPTA, we tested the intracellular Ca^{2+}-dependence of TRPC4β activation by Englerin A (10 nM). Notably, the Englerin A-evoked currents were enhanced by increasing $[Ca^{2+}]_i$ up to 1 μM, but then declined (Fig. 4*G*). While a similar biphasic response pattern to $[Ca^{2+}]_i$ had been shown for TRPC4β activation through DAMGO stimulation of μOR (Thakur *et al.* 2016), there are quantitative differences. The $[Ca^{2+}]_i$ dependence of Englerin A-evoked TRPC4β activation reached the maximum between 0.4 and 1 μM Ca^{2+}, with estimated EC_{50} values of 255 nM at −100 mV and 298 nM at +100 mV (Fig. 4*G*), instead of ~12 μM as previously determined for the μOR-mediated activation (Thakur *et al.* 2016). This difference in cytoplasmic Ca^{2+} sensitivity implies that different Ca^{2+}-regulated processes or targets may be involved between these two activation methods.

The lack of involvement of PLCδ1 in the Englerin A-evoked activation of TRPC4β may account for this difference.

More importantly, with 0.4 μM $[Ca^{2+}]_i$ buffered with BAPTA in the pipette solution, 10 nM Englerin A elicited a robust TRPC4β current in the Ca^{2+}-free bath solution that contained 1 mM EGTA and no added $CaCl_2$; however, the current was inhibited, instead of facilitated or increased, by lowering pH_i to 6.5 (Fig. 4*H* and I). These data indicate that the direct effect of intracellular protons on TRPC4 is inhibition rather than facilitation, ruling out that low pH_i accelerates $G_{i/o}$-mediated TRPC4 activation through modulation of the channel itself.

Inactivating RhoA occluded the effect of acidic pH_i on accelerating $G_{i/o}$-dependent TRPC4 activation

We then focused on whether PLCδ1 is subject to pH_i regulation. An early study using PLCδ1 proteins purified from rat brain to examine PIP_2 hydrolysis revealed a biphasic dependence on pH, which peaked at pH 6.0 and showed dramatically decreased activities at pH 5.0 and 7.2 (Kanematsu *et al.* 1992). This resembles the pH_i dependence of $G_{i/o}$-mediated TRPC4 current development shown in Fig. 3*E*, implicating that PLCδ1 may account for the dual pH_i dependence. Previously we showed that because PLCδ1 is bound and negatively regulated by the small GTPase RhoA (Hodson *et al.* 1998), the expression of a constitutively active form of RhoA (RhoA-L63, or CA-RhoA) completely abolished DAMGO-evoked TRPC4β activation (Thakur *et al.* 2016). Here, we found that lowering pH_i could not overcome the inhibitory effect of CA-RhoA (Fig. 5*B* and F), despite the obvious facilitatory effect of the low pH_i on cells that overexpressed WT RhoA (Fig. 5*A* and E). On the other hand, the activation of TRPC4β via stimulation of μOR was facilitated by the co-expression of the dominant-negative RhoA mutant, RhoA-N19, or a RhoA inhibitor, C3-exoenzyme (C3-exo), which eliminated the biphasic current development and significantly shortened T_{90} (Thakur *et al.* 2016). Interestingly, decreasing pH_i to 6.5 did not further reduce the T_{90} values in cells that expressed RhoA-N19 or C3-exo (Fig. 5*C*–F). This suggested that intracellular protons might exert their effect on TRPC4 activation through RhoA regulation of PLCδ1.

Intracellular protons increase activity of PLCδ1 in the presence of $[Ca^{2+}]_i$ elevation

To examine the effect of intracellular acidification on PLCδ1 without the confounding influence of Ca^{2+} signals arising from Ca^{2+} influx mediated by TRPC4, we assessed cellular PIP_2 levels using KCNQ2/3 channels as a readout. Voltage-dependent activation of KCNQ2/3 heteromeric channels is dependent on PIP_2 (Zhang *et al.* 2003; Li *et al.* 2005); thus, PIP_2 hydrolysis by PLC leads to a decreased KCNQ2/3 current. In μOR-expressing stable HEK293 cells transiently co-transfected with KCNQ2 and KCNQ3 and clamped under whole-cell configuration, activation of PLCs by inducing a $[Ca^{2+}]_i$ rise with IM (1 μM) led to a time-dependent decrease in the K^+ current elicited by a voltage step to 0 mV from the holding potential of −60 mV. With pH_i clamped at 7.2 using the NaAc clamp method, the IM-evoked decline of K^+ current approached the baseline in approximately 120 s, with the time for 50% decrease occurring at 30–80 s (mean ± SD, 54.3 ± 16.4 s, n = 10) after the addition of IM (Fig. 6*Aa* and D). Consistent with the involvement of PLCδ1, this response was diminished with the co-expression of a dominate-negative PLCδ1 mutant

(TagRFP-DN-PLCδ1) or CA-RhoA (Fig. 6*Ba*, Ca and D). Notably, in the absence of IM, the current was unaffected by switching the pH_i to either 7.2 or 6.5 (Fig. 6*D*), demonstrating that PLCδ1 activation, and the consequent PIP_2 hydrolysis, was triggered by the elevation of $[Ca^{2+}]_i$.

Importantly, with pH_i clamped at 6.5, the IM-induced decline in the KCNQ2/3 current became much faster than at pH_i 7.2, approaching the baseline within 30 s, with the time for 50% decrease occurring at 3.5–24.5 s (mean ± SD, 10.8 ± 7.0 s, $n = 10$, $p < 0.0001$ *vs.* pH_i 7.2) after IM application (Fig. 6*Ab* and D). This effect was markedly attenuated by the co-expression of TagRFP-DN-PLCδ1 or CA-RhoA, which not only slowed down the time course of the IM-induced current decrease but also rendered the inhibition incomplete (Fig. 6*Bb*, Cb and D). To encompass both changes, we used the currents remaining at both 30 and 120 s (I_{30}/I_0 and I_{120}/I_0) after the IM application for quantitative comparison of the different treatment conditions (Fig. 6*E*). The results clearly indicate that the Ca^{2+}-induced PIP_2 hydrolysis is mainly mediated by PLCδ1, which is negatively regulated by RhoA and strongly facilitated by the decrease in pH_i.

Furthermore, with inhibition of RhoA by the co-expression of RhoA-N19 or C3-exo, the IM-induced decline of KCNQ2/3 currents accelerated markedly as compared to the control when pH_i was clamped at 7.2 (Fig. 7*Aa*–Ca and D). The time for 50% decrease occurred at 5–43 s (mean ± SD, 22.7 ± 15.8 s, $n = 8$) and 8–47.5 s (mean ± SD, 22.9 ± 13.7 s, $n = 6$) after the addition of IM in the presence of RhoA-N19 and C3-exo, respectively. At 30 s after the IM application, the currents decreased by 67.3 ± 44.4% ($n = 9$, mean ± SD) and 73.5 ± 28.4% ($n = 6$) in cells that co-expressed RhoA-N19 and C3-exo, respectively, contrasting with the negligible decrease (mean ± SD, 2.2 ± 4.5%, $n = 8$) found in the control cells. With pH_i clamped to 6.5, all cells exhibited similar fast rates of IM-induced decline in KCNQ2/3 currents (Fig. 7*Ab*–Cb, D and E). One-way ANOVA with Tukey's multiple comparisons test indicated that pH_i 6.5 did not significantly decrease I_{30}/I_0 as compared to pH_i 7.2 in cells that co-expressed RhoA-N19 and C3-exo. However, when cells that co-expressed C3-exo were considered as an independent group, the difference between I_{30}/I_0 at pH_i 6.5 and that at pH_i 7.2 was significant by an unpaired *t* test ($p = 0.0258$, red lines in Fig. 7*E*). These data suggest that although RhoA strongly impacts the ability of PLCδ1 to sense intracellular protons, protons may still exert their effect on PLCδ1 when RhoA is inhibited.

Discussion

Although TRPC proteins have long been recognized to form Ca^{2+}-permeable receptor-operated cation channels, their mechanisms of activation remain mysterious as nearly all constituents of PLC signalling have been implicated in their gating one way or the other (Wang *et al.* 2020). For TRPC4, and partially for TRPC5 as well, the receptor-operated activation also requires an absolute involvement of PTX-sensitive $G_{i/o}$ proteins (Thakur *et al.* 2016). The dual dependence of TRPC4 gating on $G_{i/o}$ signalling and PLC makes this channel a coincident detector of two distinct G protein ($G_{i/o}$ and $G_{q/11}$) signalling pathways.

Previously, we showed that although in heterologous expression systems and renal carcinoma, TRPC4 was activatable through stimulation of $G_{i/o}$-coupled receptors in the

absence of concomitant $G_{q/11}$-PLCβ or RTK-PLCγ signalling, there was an absolute requirement on PLCδ1, as the channel activation was suppressed by any manipulations that disrupt the expression or function of this PLC isozyme (Thakur *et al.* 2016). Yet, the concomitant stimulation of the $G_{q/11}$-PLCβ or RTK-PLCγ pathway via $G_{i/o}$ signalling still exerted a kinetic effect on the TRPC4 channel by accelerating the activation rate. The main difference between PLCδ1 and other PLC isozymes is that whereas PLCδ1 is dependent solely on Ca^{2+} for activation, others, especially PLCβs and PLCγs, typically rely on other triggers, such as receptor stimulation, to enter the active state in addition to Ca^{2+}. It may be viewed that the Ca^{2+} sensitivities of different PLC isozymes are subject to change by other factors, such as G$\alpha_{q/11}$-GTP for PLCβs or tyrosine phosphorylation for PLCγ. Hence, the activation of PLCβs or PLCγs by respective ligands/receptors probably facilitates TRPC4 opening through promoting PLCδ1, the prototypical PLC isozyme with Ca^{2+} as the main stimulus without any other known trigger. However, mimicking receptor-evoked $[Ca^{2+}]_i$ elevation with IM, which when used at 1 μM also mobilizes ER Ca^{2+} and triggers store-operated Ca^{2+} entry, only improved the probability, but not kinetics, of $G_{i/o}$-mediated and PLCδ1-dependent TRPC4 activation (Thakur *et al.* 2016), suggesting the presence of a rate-limiting factor(s) in $G_{q/11}$-PLCβ and RTK-PLCγ signalling that is lacking in IM-stimulated $[Ca^{2+}]_i$ elevation. Such a factor may be a common product of the PLC pathway as the $G_{i/o}$-mediated TRPC4 activation was accelerated by stimulating either PLCβs or PLCγs (Thakur *et al.* 2016). It is likely that this factor is produced by PLCδ1 as well.

Here, we show that this factor is H^+, a known byproduct of PIP_2 hydrolysis. It was estimated that under neutral pH, the hydrolysis of each PIP_2 molecule by PLC produces 0.8 protons (Huang *et al.* 2015). This may not be much globally as even in *Drosophila* photoreceptors, where receptors and G proteins are highly packed in the rhabdomere, the light-induced PLC activation only decreased pH_i by 0.2 pH units (Huang *et al.* 2015). However, the local pH change must be quite significant when a large number of PIP_2 molecules are simultaneously hydrolysed, as in the case of receptor agonist-evoked $G_{q/11}$-PLCβ or RTK-PLCγ activation. Our data that the CCh facilitation was suppressed by an internal solution buffered with 100 mM, but not 10 mM, Hepes (Fig. 2*C*–E) support the idea that the proton effect is local. Nonetheless, PIP_2 hydrolysis may not be the only source of proton production associated with PLC activity; other sources such as intracellular membranes or organelles might also contribute to proton generation.

Because PLCδ1 is both a generator and the sensor of the protons, its activation becomes self-propagating through positive feedback, such that the activation of a few PLCδ1 molecules eventually may recruit all PLCδ1 into activation (Fig. 7*F*). However, in the early phase of $G_{i/o}$ stimulation, the number of active PLCδ1 molecules must be too low to generate sufficient local pH drop to trigger widespread PLCδ1 activation, creating the typical pace-making phase of TRPC4 current development, until the number of activated PLCδ1 molecules became sufficient to support continued global activation of the enzyme, and in turn TRPC4, leading to the rapid current increase in the later phase. We show that by lowering the global pH_i to around 6.5 using several different methods, the pace-making phase was eliminated and the $G_{i/o}$-mediated activation was accelerated to the same extent as the co-stimulation with $G_{q/11}$-PLCβs.

Importantly, lowering pH_i alone does not accelerate $G_{i/o}$-mediated TRPC4 activation. $[Ca^{2+}]_i$ elevation is necessary (Fig. 7*F*). There are multiple sources of Ca^{2+}: ER Ca^{2+} release through IP_3 receptors or IM and Ca^{2+} influx through endogenous store-operated channels as well as the activated TRPC4 channels. In the early phase, the limited PLCδ1 activity led not only to insufficient pH_i drop but also to a Ca^{2+} signal that was too weak to support more widespread PLCδ1 activation. This explains why the low pH_i-mediated acceleration was only detected in the presence, but not absence, of IM (Fig. 3*E*), as in the absence of IM Ca^{2+} also became limiting. Our data thus reveal a very interesting aspect of PLCδ1 regulation that requires simultaneous increases in the concentrations of both H^+ and Ca^{2+} in the vicinity of the enzyme (Fig. 7*F*). Remarkably, stimulation of other PLC isozymes with receptor agonists, for instance PLCβs or PLCγs, fulfils both requirements and is therefore able to markedly accelerate PLCδ1 activation and in turn TRPC4 current development, when there is also coincident $G_{i/o}$ stimulation (Fig. 7*F*).

Our assertation that H^+ acts at PLCδ1, instead of the channel, to accelerate TRPC4 current development is also supported by the findings that (1) low pH_i is inhibitory to the channel when it is activated by its direct agonist, Englerin A (Fig. 4*H* and I), and (2) the Ca^{2+}-induced PLCδ1-mediated hydrolysis of PIP_2, as assessed using KCNQ2/3, is accelerated by lowering pH_i in the absence of TRPC4 (Figs 6 and 7). Moreover, although both PLCδ1 and TRPC4 require a rise in $[Ca^{2+}]_i$ for activation, the required concentration ranges appear to be different. While the PLC-independent activation of TRPC4 caused by Englerin A displayed a high sensitivity (EC_{50} = 255–298 nM, Fig. 4*G*) to $[Ca^{2+}]_i$, the PLCδ1-dependent channel activation through stimulation of co-expressed μOR required >5 μM free cytosolic Ca^{2+} (Thakur *et al.* 2016). The higher $[Ca^{2+}]_i$ requirement for the $G_{i/o}$-mediated TRPC4 activation than that evoked by Englerin A probably reflects the Ca^{2+} dependence of PLCδ1, instead of TRPC4. In such a case, PLCδ1 sets the rate limit on $G_{i/o}$-mediated TRPC4 activation due to its dual dependence on both intracellular H^+ and Ca^{2+}, two factors that underlie the self-propagating feature of this enzyme (Fig. 7*F*).

Early biochemical analysis revealed an optimal pH of 6.0 for PLCδ1 isolated from rat brain (Kanematsu *et al.* 1992). However, the reported optimal pH for PLCδ-like proteins purified from bovine or rat brain, or rat liver, ranged from 5.5 to 7.1 by different groups (Ryu *et al.* 1987; Fukui *et al.* 1988; Homma *et al.* 1988), suggesting that the pH sensitivity may vary between different PLC isozymes and/or according to experimental conditions. Although the pH dependence of PLCδ1 in intact cells may differ from those obtained from studying the purified proteins, our current finding of the pH_i required to support $G_{i/o}$-mediated TRPC4 activation (pH 6.25–7.0) falls well within the pH range for optimal activities of purified PLCδ proteins. This further supports the notion that PLCδ1 is the proton sensor that limits the rate of $G_{i/o}$ activation of TRPC4 channels.

Our data also indicate that RhoA can limit the effect of protons. Both TRPC4-dependent (Fig. 5) and TRPC4-independent (Fig. 6) activation of PLCδ1 was suppressed by the constitutive activation of RhoA and, only for the TRPC4-independent activation, low pH_i partially overcame the suppression (Fig. 6). On the other hand, inhibiting RhoA not only markedly accelerated Ca^{2+}-induced activation of PLCδ1, detected based on both $G_{i/o}$-mediated TRPC4 activation (Fig. 5) and inhibition of KCNQ2/3 currents (Fig. 7), but also

largely precluded further actions of the low pH_i. It may be possible that protons could interfere with RhoA binding to PLCδ1 and thereby free PLCδ1 from the tonic inhibition. However, given that the purified PLCδ had moderately acidic optimal pH in biochemical experiments (Kanematsu *et al.* 1992) and low pH_i tended to further increase the rate of IM-induced decline of KCNQ2/3 currents when RhoA was inhibited (Fig. 7), it is likely that intracellular protons act directly on PLCδ1, although it cannot be ruled out that protons may also facilitate Ca^{2+}-dependent PLCδ1 activation by disrupting RhoA binding and thereby its inhibition.

Even though PLCδ1 underlies the actual PLC dependence of TRPC4 activation in response to $G_{i/o}$ stimulation (Thakur *etal.* 2016), this PLC isozyme may not fulfil a true signalling role in that it is not readily activated by any environmental cues like PLCβs or PLCγs, which are activated by receptor-coupled $G_{q/11}$ signalling or RTKs, respectively. In this regard, unless conditions are met for spontaneous PLCδ1 activation, the receptor-operated TRPC4 channel opening needs to be initiated by coincident stimulation of $G_{i/o}$ with either $G_{q/11}$-PLCβs or RTK-PLCγs. Indeed, for the native TRPC4-containing channels in gastrointestinal smooth muscle cells that receive cholinergic inputs from parasympathetic nerves (Tsvilovskyy *et al.* 2009), the activation is dependent on the co-stimulation of both $G_{i/o}$ and $G_{q/11}$-coupled M2 and M3 muscarinic receptors, respectively (Zholos & Bolton, 1997). Other TRPC4-like native responses, detected as either Ca^{2+} influx or membrane depolarization, tend to be elicited through stimulation of $G_{q/11}$-coupled receptors (Phelan *et al.* 2013; Riccio *et al.* 2014; Tian *et al.* 2014*b*). Future studies should address the possibility of unintentional coincident activation of $G_{i/o}$ signalling under the experimental conditions used before assuming these to be purely $G_{q/11}$-PLCβ-mediated TRPC4 activation. On the other hand, the rarity of detecting purely $G_{i/o}$-mediated TRPC4-like current or membrane depolarization responses in native systems could be attributed to either the lack of simultaneous $G_{q/11}$-PLCβ or RTK-PLCγ signalling or intracellular Ca^{2+} signals combined with acidification. However, given that $[Ca^{2+}]_i$ increase and acidosis are events that typically coincide in smooth muscle cells and the cardio-pulmonary vasculature during hypoxic and ischaemic conditions, as well as in neurons during brain injury and epileptic attack (Taggart & Wray, 1998; Lipton, 1999; Ladilov *et al.* 2000), the normally inhibitory $G_{i/o}$ signalling may become excessively excitatory through the activation of TRPC4. Indeed, a number of studies have shown an upregulation of TRPC4 in hypoxic conditions (Alzoubi *et al.* 2013; Parrau *et al.* 2013) and the involvement of TRPC4 in neuronal death (Phelan *et al.* 2013). It is imperative to consider acidosis as a contributing factor of membrane excitation resulting from enhanced $G_{i/o}$ signalling and the involvement of TRPC4-containing channels for such an effect.

In summary, we show here that Ca^{2+} and H^+ act cooperatively from the cytoplasmic side to induce the activation of PLCδ1, through which they support TRPC4 gating in the presence of $G_{i/o}$ signalling. Because simultaneous pH_i drop and $[Ca^{2+}]_i$ elevation are normally provided through ligand stimulation of the $G_{q/11}$-PLCβ or RTK-PLCγ pathways, this requirement makes TRPC4-containing channels excellent coincident sensors of $G_{i/o}$ and $G_{q/11}$ (or RTK) signalling. However, under stress conditions with tissue acidosis, and the consequent intracellular acidification, the channels can become responsive to just $[Ca^{2+}]_i$ rise and $G_{i/o}$ signalling, resulting in extended membrane depolarization and intracellular

Ca^{2+} overload that damage the cell. The cell-damaging effect may be further exacerbated given that the activities of PLCδ1 and TRPC4 are self-propagating because they act as both the sensors and the generators of the Ca^{2+} signal. For PLCδ1, this also holds true for protons. Interestingly, both H^+ and Ca^{2+} work within a rather narrow concentration range, revealing an extremely tight regulation on TRPC4 function. These findings not only enrich our mechanistic understanding of how $G_{i/o}$ and $G_{q/11}$ co-stimulation contributes to receptor-operated TRPC4 activation and further strengthen the critical involvement of PLCδ1 in TRPC4 gating, but also shed new lights on how TRPC4-containing channels can contribute to normal physiology and disease.

Acknowledgements

We are grateful to Drs Y. Okamura, J. Frost and M. Shapiro for providing the cDNA constructs used in this study. We thank Mr Nicholas E. Karagas (University of Texas Health Science Center at Houston) for critical reading and helpful comments on the manuscript.

Funding

This research was supported in part by NIH grants (DK081654 and NS092377 to M.X.Z.), an American Heart Association predoctoral fellowship (13PRE17200004 to D.P.T.) and a postdoc fellowship (17POST33661282 to Q.W.).

Biographies

Dhananjay Thakur earned his PhD degree at the University of Texas Health Science Center in Houston under Dr Michael Zhu, working on the gating mechanisms of TRP channels. He is now a postdoc at UC Santa Barbara working with Dr Craig Montell, where he is building optogenetic tools and dissecting mechanisms of sensory integration in *Drosophila*. In the future, he aims to continue building tools for neuroscience while investigating mechanisms of neuronal computation.

Qiaochu Wang earned his PhD from the Institute of Zoology, Chinese Academy of Sciences, under Dr Tie-Shan Tang, where he characterized a novel Ca^{2+} release channel from endoplasmic reticulum. He then had his postdoc training with Dr Michael Zhu in Houston, where he acquired electrophysiological and other skills for studying channels on plasma membrane and intracellular organelles. He is now Associate Professor in Beijing

Children's Hospital, investigating deregulation of ion homeostasis in melanosomes that underlies albinism.

References

Akbulut Y, Gaunt HJ, Muraki K, Ludlow MJ, Amer MS, Bruns A, Vasudev NS, Radtke L, Willot M, Hahn S, Seitz T, Ziegler S, Christmann M, Beech DJ & Waldmann H (2015). (–)-Englerin A is a potent and selective activator of TRPC4 and TRPC5 calcium channels. Angew Chem Int Ed Engl 54, 3787–3791. [PubMed: 25707820]

Alzoubi A, Almalouf P, Toba M, O'Neill K, Qian X, Francis M, Taylor MS, Alexeyev M, McMurtry IF, Oka M & Stevens T (2013). TRPC4 inactivation confers a survival benefit in severe pulmonary arterial hypertension. Am J Pathol 183, 1779–1788. [PubMed: 24113457]

Blair NT, Kaczmarek JS & Clapham DE (2009). Intracellular calcium strongly potentiates agonist-activated TRPC5 channels. J Gen Physiol 133, 525–546. [PubMed: 19398778]

Clapham DE (2003). TRP channels as cellular sensors. Nature 426, 517–524. [PubMed: 14654832]

Foskett JK, White C, Cheung KH & Mak DO (2007). Inositol trisphosphate receptor Ca^{2+} release channels. Physiol Rev 87, 593–658. [PubMed: 17429043]

Fukui T, Lutz RJ & Lowenstein JM (1988). Purification of a phospholipase C from rat liver cytosol that acts on phosphatidylinositol 4,5-bisphosphate and phosphatidylinositol 4-phosphate. J Biol Chem 263, 17730–17737. [PubMed: 2846577]

Gao L, Yang P, Qin P, Lu Y, Li X, Tian Q, Li Y, Xie C, Tian JB, Zhang C, Tian C, Zhu MX & Yao J (2016). Selective potentiation of 2-APB-induced activation of TRPV1–3 channels by acid. Sci Rep 6, 20791. [PubMed: 26876731]

Garcia P, Gupta R, Shah S, Morris AJ, Rudge SA, Scarlata S, Petrova V, McLaughlin S & Rebecchi MJ (1995). The pleckstrin homology domain of phospholipase C-delta 1 binds with high affinity to phosphatidylinositol 4,5-bisphosphate in bilayer membranes. Biochemistry 34, 16228–16234. [PubMed: 8519781]

Hodson EA, Ashley CC, Hughes AD & Lymn JS (1998). Regulation of phospholipase C-delta by GTP-binding proteins-rhoA as an inhibitory modulator. Biochim Biophys Acta 1403, 97–101. [PubMed: 9622602]

Hofmann T, Obukhov AG, Schaefer M, Harteneck C, Gudermann T & Schultz G (1999). Direct activation of human TRPC6 and TRPC3 channels by diacylglycerol. Nature 397, 259–263. [PubMed: 9930701]

Homma Y, Imaki J, Nakanishi O & Takenawa T (1988). Isolation and characterization of two different forms of inositol phospholipid-specific phospholipase C from rat brain. J Biol Chem 263, 6592–6598. [PubMed: 3360794]

Huang J, Liu CH, Hughes SA, Postma M, Schwiening CJ & Hardie RC (2010). Activation of TRP channels by protons and phosphoinositide depletion in *Drosophila* photoreceptors. Curr Biol 20, 189–197. [PubMed: 20116246]

Jeon JP, Hong C, Park EJ, Jeon JH, Cho NH, Kim IG, Choe H, Muallem S, Kim HJ & So I (2012). Selective $G\alpha i$ subunits as novel direct activators of transient receptor potential canonical (TRPC)4 and TRPC5 channels. J Biol Chem 287, 17029–17039. [PubMed: 22457348]

Jeon JP, Thakur DP, Tian JB, So I & Zhu MX (2016). Regulator of G-protein signalling and GoLoco proteins suppress TRPC4 channel function via acting at $G\alpha_{i/o}$. Biochem J 473, 1379–1390. [PubMed: 26987813]

Kanematsu T, Takeya H, Watanabe Y, Ozaki S, Yoshida M, Koga T, Iwanaga S & Hirata M (1992). Putative inositol 1,4,5-trisphosphate binding proteins in rat brain cytosol. J Biol Chem 267, 6518–6525. [PubMed: 1313009]

Kim H, Jeon JP, Hong C, Kim J, Myeong J, Jeon JH & So I (2013). An essential role of $PI_{4,5}P_2$ for maintaining the activity of the transient receptor potential canonical (TRPC)4beta. Pflugers Arch 465, 1011–1021. [PubMed: 23417604]

Kiselyov K, Xu X, Kuo TH, Mozhayeva G, Pessah I, Mignery G, Zhu X, Birnbaumer L & Muallem S (1998). Functional interaction between InsP3 receptors and store-operated Htrp3 channels. Nature 396, 478–482. [PubMed: 9853757]

Ladilov Y, Schafer C, Held A, Schafer M, Noll T & Piper HM (2000). Mechanism of Ca^{2+} overload in endothelial cells exposed to simulated ischemia. Cardiovasc Res 47, 394–403. [PubMed: 10946076]

Lemonnier L, Trebak M & Putney JW Jr (2008). Complex regulation of the TRPC3, 6 and 7 channel subfamily by diacylglycerol and phosphatidylinositol-4,5-bisphosphate. Cell Calcium 43, 506–514. [PubMed: 17942152]

Li Y, Gamper N, Hilgemann DW & Shapiro MS (2005). Regulation of Kv7 (KCNQ) K^+ channel open probability by phosphatidylinositol 4,5-bisphosphate. J Neurosci 25, 9825–9835. [PubMed: 16251430]

Lipton P (1999). Ischemic cell death in brain neurons. Physiol Rev 79, 1431–1568. [PubMed: 10508238]

Lomasney JW, Cheng HF, Wang LP, Kuan Y, Liu S, Fesik SW & King K (1996). Phosphatidylinositol 4,5-bisphosphate binding to the pleckstrin homology domain of phospholipase C-delta1 enhances enzyme activity. J Biol Chem 271, 25316–25326. [PubMed: 8810295]

Miller M, Shi J, Zhu Y, Kustov M, Tian JB, Stevens A, Wu M, Xu J, Long S, Yang P, Zholos AV, Salovich JM, Weaver CD, Hopkins CR, Lindsley CW, McManus O, Li M & Zhu MX (2011). Identification of ML204, a novel potent antagonist that selectively modulates native TRPC4/C5 ion channels. J Biol Chem 286, 33436–33446. [PubMed: 21795696]

Murthy KS, Zhou H, Huang J & Pentyala SN (2004). Activation of PLC-δ1 by $G_{i/o}$-coupled receptor agonists. Am J Physiol Cell Physiol 287, C1679–C1687. [PubMed: 15525688]

Niemeyer MI, Cid LP, Pena-Munzenmayer G & Sepulveda FV (2010). Separate gating mechanisms mediate the regulation of K2P potassium channel TASK-2 by intra- and extracellular pH. J Biol Chem 285, 16467–16475. [PubMed: 20351106]

Otsuguro K, Tang J, Tang Y, Xiao R, Freichel M, Tsvilovskyy V, Ito S, Flockerzi V, Zhu MX & Zholos AV (2008). Isoform-specific inhibition of TRPC4 channel by phosphatidylinositol 4,5-bisphosphate. J Biol Chem 283, 10026–10036. [PubMed: 18230622]

Parrau D, Ebensperger G, Herrera EA, Moraga F, Riquelme RA, Ulloa CE, Rojas RT, Silva P, Hernandez I, Ferrada J, Diaz M, Parer JT, Cabello G, Llanos AJ & Reyes RV (2013). Store-operated channels in the pulmonary circulation of high- and low-altitude neonatal lambs. Am J Physiol Lung Cell Mol Physiol 304, L540–L548. [PubMed: 23418093]

Phelan KD, Shwe UT, Abramowitz J, Wu H, Rhee SW, Howell MD, Gottschall PE, Freichel M, Flockerzi V, Birnbaumer L & Zheng F (2013). Canonical transient receptor channel 5 (TRPC5) and TRPC1/4 contribute to seizure and excitotoxicity by distinct cellular mechanisms. Mol Pharmacol 83, 429–438. [PubMed: 23188715]

Plant TD & Schaefer M (2003). TRPC4 and TRPC5: receptor-operated Ca^{2+}-permeable nonselective cation channels. Cell Calcium 33, 441–450. [PubMed: 12765689]

Randall AS, Liu CH, Chu B, Zhang Q, Dongre SA, Juusola M, Franze K, Wakelam MJ & Hardie RC (2015). Speed and sensitivity of phototransduction in Drosophila depend on degree of saturation of membrane phospholipids. J Neurosci 35, 2731–2746. [PubMed: 25673862]

Rhee SG & Bae YS (1997). Regulation of phosphoinositide-specific phospholipase C isozymes. J Biol Chem 272, 15045–15048. [PubMed: 9182519]

Riccio A, Yan L, Tsvetkov E, Gapon S, Gui LY, Smith KS, Engin E, Rudolph U, Bolshakov VY & Clapham DE (2014). Decreased anxiety-like behavior and $G\alpha_{q/11}$-dependent responses in the amygdala of mice lacking TRPC4 channels. J Neurosci 34, 3653–3667. [PubMed: 24599464]

Ryu SH, Suh PG, Cho KS, Lee KY & Rhee SG (1987). Bovine brain cytosol contains three immunologically distinct forms of inositolphospholipid-specific phospholipase C. Proc Natl Acad Sci U S A 84, 6649–6653. [PubMed: 3477795]

Salvi A, Quillan JM & Sadée W (2002). Monitoring intracellular pH changes in response to osmotic stress and membrane transport activity using 5-chloromethylfluorescein. AAPS PharmSci 4, 21–28.

Semtner M, Schaefer M, Pinkenburg O & Plant TD (2007). Potentiation of TRPC5 by protons. J Biol Chem 282, 33868–33878. [PubMed: 17884814]

Shi J, Mori E, Mori Y, Mori M, Li J, Ito Y & Inoue R (2004). Multiple regulation by calcium of murine homologues of transient receptor potential proteins TRPC6 and TRPC7 expressed in HEK293 cells. J Physiol 561, 415–432. [PubMed: 15579537]

Storch U, Forst AL, Pardatscher F, Erdogmus S, Philipp M, Gregoritza M, Mederos Y, Schnitzler M & Gudermann T (2017). Dynamic NHERF interaction with TRPC4/5 proteins is required for channel gating by diacylglycerol. Proc Natl Acad Sci U S A 114, E37–E46. [PubMed: 27994151]

Taggart MJ & Wray S (1998). Hypoxia and smooth muscle function: key regulatory events during metabolic stress. J Physiol 509, 315–325. [PubMed: 9575282]

Thakur DP, Tian JB, Jeon J, Xiong J, Huang Y, Flockerzi V & Zhu MX (2016). Critical roles of $G_{i/o}$ proteins and phospholipase C-delta1 in the activation of receptor-operated TRPC4 channels. Proc Natl Acad Sci U S A 113, 1092–1097. [PubMed: 26755577]

Tian J, Thakur DP & Zhu MX (2014a). TRPC channels In Handbook of Ion Channels, eds. Zheng J & Trudeau MC, pp. 411–426. CRC Press, Boca Raton, FL.

Tian J, Thakur DP, Lu Y, Zhu Y, Freichel M, Flockerzi V & Zhu MX (2014b). Dual depolarization responses generated within the same lateral septal neurons by TRPC4-containing channels. Pflugers Arch 466, 1301–1316. [PubMed: 24121765]

Trebak M, Lemonnier L, DeHaven WI, Wedel BJ, Bird GS & Putney JW Jr (2009). Complex functions of phosphatidylinositol 4,5-bisphosphate in regulation of TRPC5 cation channels. Pflugers Arch 457, 757–769. [PubMed: 18665391]

Tsvilovskyy VV, Zholos AV, Aberle T, Philipp SE, Dietrich A, Zhu MX, Birnbaumer L, Freichel M & Flockerzi V (2009). Deletion of TRPC4 and TRPC6 in mice impairs smooth muscle contraction and intestinal motility in vivo. Gastroenterology 137, 1415–1424 [PubMed: 19549525]

Venkatachalam K & Montell C (2007). TRP channels. Annu Rev Biochem 76, 387–417. [PubMed: 17579562]

Wang YZ, Wang JJ, Huang Y, Liu F, Zeng WZ, Li Y, Xiong ZG, Zhu MX & Xu TL (2015). Tissue acidosis induces neuronal necroptosis via ASIC1a channel independent of its ionic conduction. Elife 4, pii: e05682. [PubMed: 26523449]

Wang H, Cheng X, Tian J, Xiao Y, Tian T, Xu F, Hong X & Zhu MX (2020). TRPC channels: Structure, function, regulation and recent advances in small molecular probes. Pharmacol Ther 28, 107497 10.1016/j.pharmthera.2020.107497.

Yuan Y, Shimura M & Hughes BA (2003). Regulation of inwardly rectifying K^+ channels in retinal pigment epithelial cells by intracellular pH. J Physiol 549, 429–438. [PubMed: 12665599]

Zhang Z, Tang J, Tikunova S, Johnson JD, Chen Z, Qin N, Dietrich A, Stefani E, Birnbaumer L & Zhu MX (2001). Activation of Trp3 by inositol 1,4,5-trisphosphate receptors through displacement of inhibitory calmodulin from a common binding domain. Proc Natl Acad Sci U S A 98, 3168–3173. [PubMed: 11248050]

Zhang H, Craciun LC, Mirshahi T, Rohács T, Lopes CMB, Jin T & Logothetis DE (2003). PIP_2 activates KCNQ channels, and its hydrolysis underlies receptor-mediated inhibition of M currents. Neuron 37, 963–975. [PubMed: 12670425]

Zholos AV & Bolton TB (1997). Muscarinic receptor subtypes controlling the cationic current in guinea-pig ileal smooth muscle. Br J Pharmacol 122, 885–893. [PubMed: 9384504]

Key points

- Receptor-operated activation of TRPC4 cation channels requires $G_{i/o}$ proteins and phospholipase-Cδ1 (PLCδ1) activation by intracellular Ca^{2+}.
- Concurrent stimulation of the $G_{q/11}$ pathway accelerates $G_{i/o}$ activation of TRPC4, which is not mimicked by increasing cytosolic Ca^{2+}.
- The kinetic effect of $G_{q/11}$ was diminished by alkaline intracellular pH (pH_i) and increased pH_i buffer capacity.
- Acidic pH_i (6.75–6.25) together with the cytosolic Ca^{2+} rise accelerated $G_{i/o}$-mediated TRPC4 activation.
- Protons exert their facilitation effect through Ca^{2+}-dependent activation of PLCδ1.
- The data suggest that the $G_{q/11}$-PLCβ pathway facilitates $G_{i/o}$ activation of TRPC4 through hydrolysing phosphatidylinositol 4,5-bisphosphate (PIP_2) to produce the initial proton signal that triggers a self-propagating PLCδ1 activity supported by regenerative H^+ and Ca^{2+}.
- The findings provide novel mechanistic insights into receptor-operated TRPC4 activation by coincident $G_{q/11}$ and $G_{i/o}$ pathways and shed light on how aberrant activation of TRPC4 may occur under pathological conditions to cause cell damage.

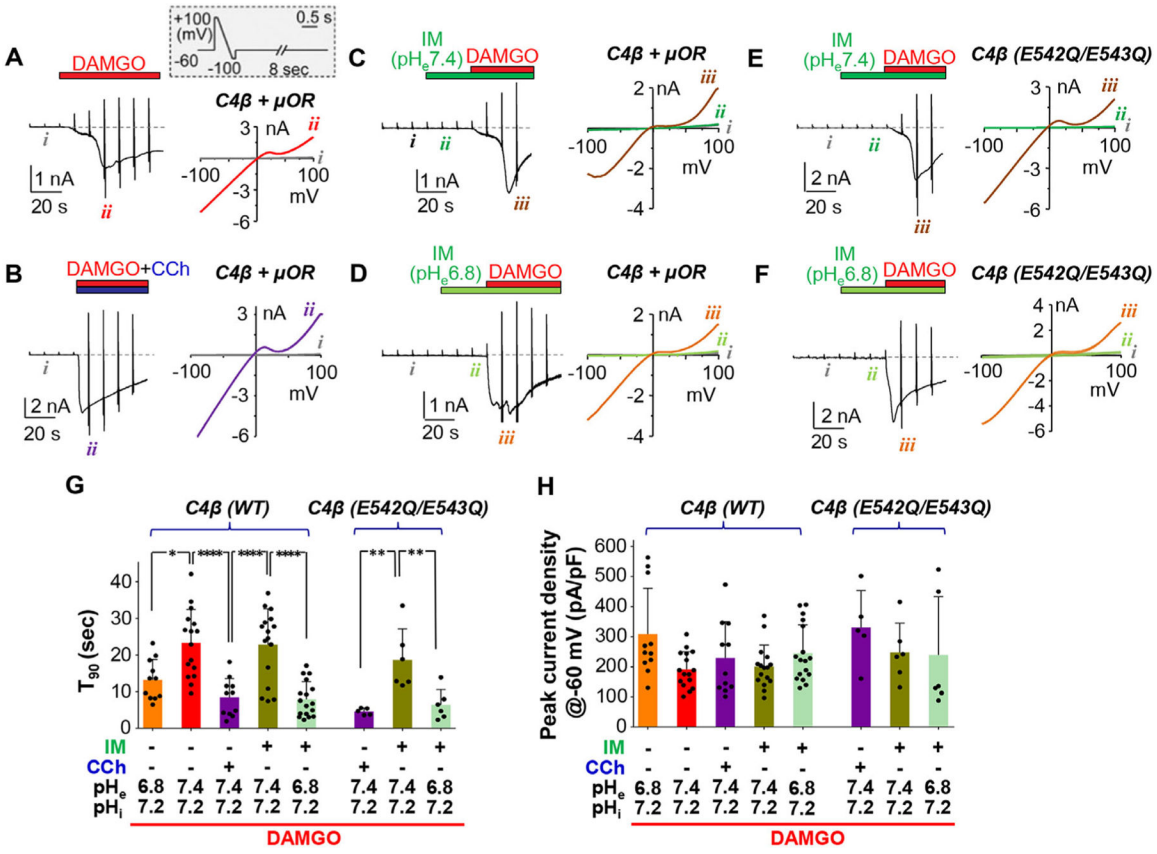

Figure 1. Acidic pH accelerates the rate of $G_{i/o}$ mediated-TRPC4 activation

A–D, HEK293 cells stably co-expressing mouse TRPC4*β* and *μ*OR were voltage clamped in whole-cell mode with the pipette solution containing 0.05 mM EGTA and 10 mM Hepes to buffer Ca^{2+} and H^+, respectively. The bath solution contained 2 mM Ca^{2+}. Voltage protocol is shown in inset to *A*. Left panels show representative time courses of currents at −60 mV; right panels show *I–V* relationships obtained by the voltage ramp at the indicated time points. Cells were stimulated with 1 μM DAMGO alone (*A*), 1 μM DAMGO plus 10 μM CCh (*B*), or 1 μM DAMGO with IM added in a pH 7.4 (*C*) or pH 6.8 (*D*) extracellular solution at 30 s before DAMGO, as indicated by the horizontal bars above the current traces. Drug names (DAMGO, red; IM, green; CCh, blue) are colour-coded throughout in all figure panels. Vertical strikes in the traces resulted from the voltage ramp. *E* and *F*, similar to *C* and *D* but HEK293 cells stably expressing *μ*OR were transiently transfected with TRPC4*β* mutant, E542Q/E543Q. *G*, summary of time required for the current to develop to 90% of the maximum after DAMGO application (T_{90}) under various conditions as indicated. *H*, summary of *A–F* for peak current density at −60 mV evoked by DAMGO. Columns and error bars are means ± SD. Dots show data points of individual cells. *$p < 0.05$, **$p < 0.01$, ***$p < 0.001$, ****$p < 0.0001$, by one-way ANOVA with Tukey's multiple comparisons test.

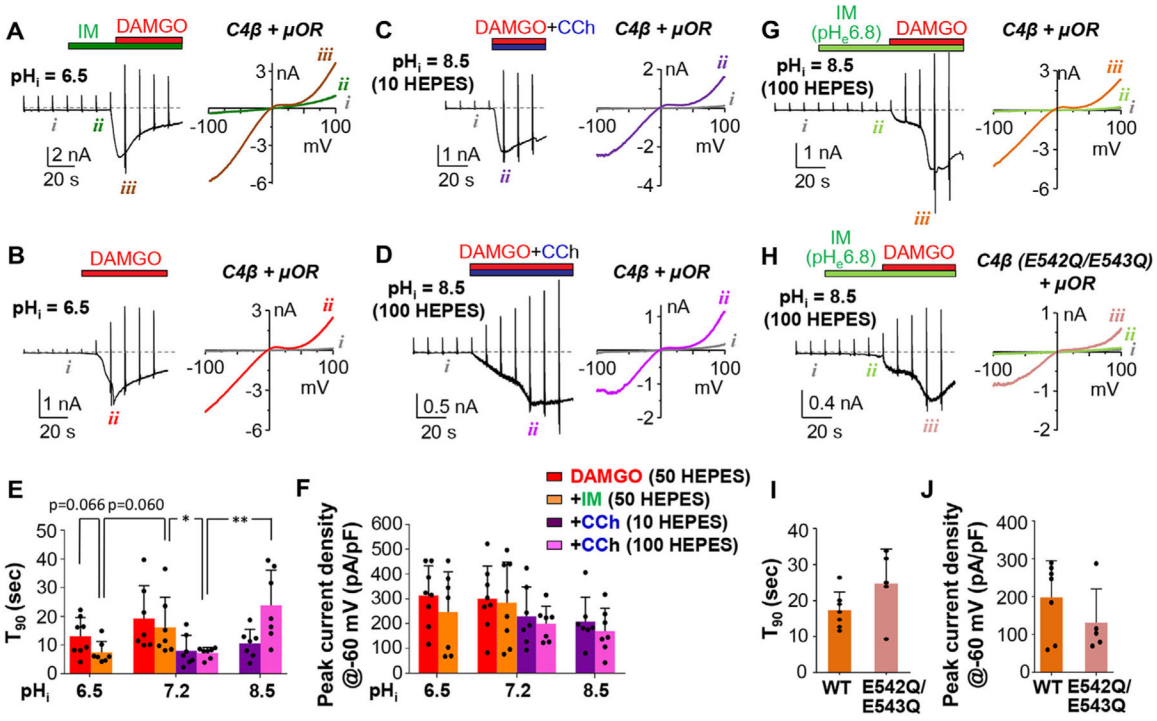

Figure 2. Intracellular pH affects the rate of $G_{i/o}$-mediated TRPC4 activation

A–D, cells stably co-expressing TRPC4*β* and *μ*OR were used. For *A* and *B*, the pipette solution contained 0.05 mM EGTA and pH_i was buffered to 6.5 by 50 mM Hepes. For *C* and *D*, the pipette solutions contained 0.05 mM EGTA and pH_i was buffered to 8.5 with either 10 (*C*) or 100 mM (*D*) Hepes. Cells were stimulated with DAMGO (1 μM), IM (1 μM) and CCh (10 μM) in pH 7.4 solution as indicated. *E* and *F*, summary of T_{90} (*E*) and peak current density at −60 mV (*F*) for the conditions indicated. Voltage protocols and display conventions follow that of Fig. 1. $*p < 0.05$, $**p < 0.01$, by one-way ANOVA with Tukey's multiple comparisons test. *G* and *H*, example current traces of HEK293 cells stably expressing *μ*OR and transiently transfected with cDNA for wild type (*G*) or the E542Q/E543Q mutant (*H*) of TRPC4*β*. The pipette solution contained 0.05 mM EGTA and the pH_i was buffered at 8.5 with 100 mM Hepes. Cells were stimulated with IM and DAMGO with the extracellular pH at 6.8. *I* and *J*, summary of T_{90} (*I*) and peak current density at −60 mV (*J*) for the conditions shown in *G* and *H*.

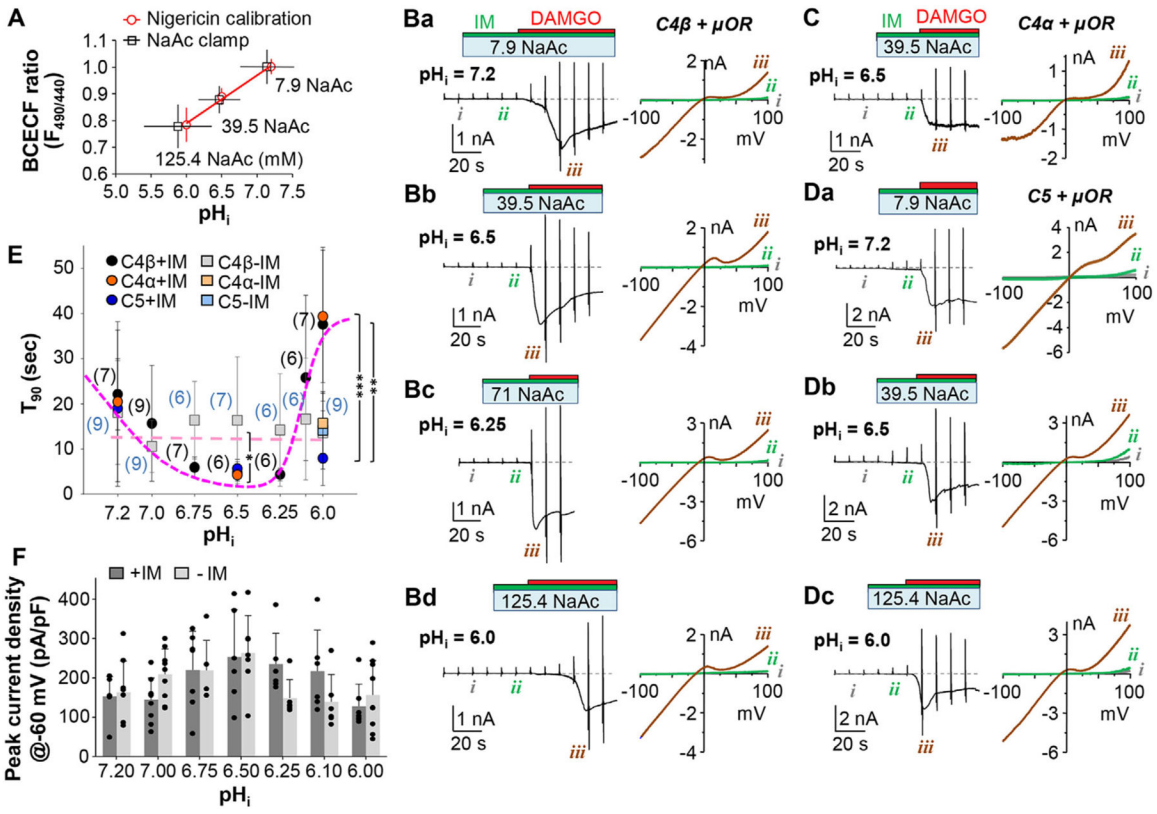

Figure 3. Intracellular acidification accelerates the rates of $G_{i/o}$-mediated activation of TRPC4 and TRPC5 in a Ca^{2+}-dependent manner

A, pH_i measurement under similar conditions as for whole-cell recording of TRPC4 currents. The pipette solution contained 5 mM NaAc and 300 μM BCECF. Fluorescence ratios ($F_{490/440}$) of BCECF were obtained with extracellular NaAc being 7.9, 39.5 or 125.4 mM (NaAc clamp, black squares), or with extracellular solutions of defined pH of 7.2, 6.5 and 6.0 in the presence of 10 μM nigericin (Nigericin calibration, red circles). Data are means ± SD (n = 5). pH_i values for NaAc clamp were determined based on the BCECF ratios and nigericin calibration for each experiment. *B–D*, representative time courses of currents at −60 mV (left panels) and *I–V* curves for the indicated conditions (right panels) of HEK293 cells stably co-expressing μOR with TRPC4β (*Ba–Bd*), TRPC4α (*C*) or TRPC5 (*Da–Dc*). The pipette solution contained 0.05 mM EGTA and 5 mM NaAc, pH 7.4. To alter pH_i, different concentrations of NaAc (in mM) were bath applied with 1 μM IM at pH 7.4 prior to the addition of 1 μM DAMGO as indicated. Note the differences in the kinetics of current development with different pH_i. *E*, summary (means ± SD) of T_{90} for DAMGO-evoked currents in the presence (circles) and absence (squares) of IM with pH_i changed by NaAc for cells that stably expressed μOR together with TRPC4β, TRPC4α or TRPC5. For TRPC4β, numbers of cells (n) are indicated in parentheses (black, with IM; blue, without IM). For TRPC4α with IM, n = 9, 6 and 7 cells, TRPC5 with IM, n = 6, 6 and 8 cells, at pH_i 7.2, 6.5 and 6.0, respectively. For TRPC4α without IM at pH_i 6.0, n = 6 cells, and for TRPC5 without IM at pH_i 6.0, n = 7. Note the lack of inhibition by pH 6.0 for TRPC5. Data for TRPC4β in the presence of IM were fitted with the biphasic Hill equation assuming maximal and minimal T_{90} values of 50 and 3.3 s. The estimated EC_{50} for pH_i facilitation

was 7.25, Hill 2.15; the estimated IC_{50} for pH_i inhibition was 6.09, Hill −7.07. Data for TRPC4β in the absence of IM were fitted with linear regression. *$p < 0.05$ for +IM *vs.* −IM for TRPC4β at pH_i 6.5 by unpaired *t* test; **$p < 0.01$, ***$p < 0.001$ for TRPC4β and TRPC4α *vs.* TRPC5 (+IM) at pH_i 6.0, by unpaired *t* test. *F*, summary (means ± SD) of peak TRPC4β current density at −60 mV evoked by DAMGO in the presence (dark grey) and absence (light grey) of IM with pH_i changed by NaAc to values as indicated.

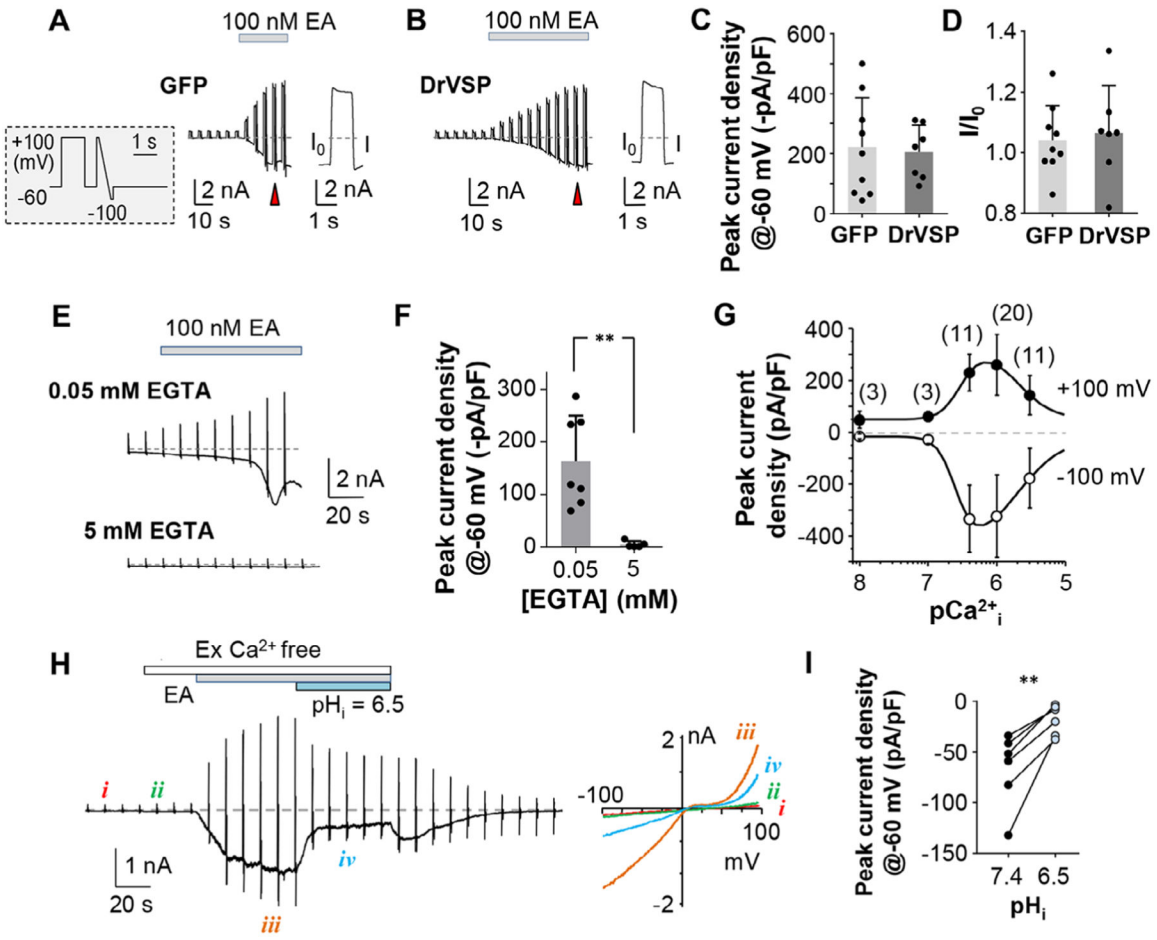

Figure 4. Intracellular acidification inhibits TRPC4 current evoked by its direct agonist, Englerin A

A–D, Englerin A (EA)-evoked TRPC4 current is independent of PIP_2. Cells stably co-expressing μOR and TRPC4β were transiently transfected with either a control vector (GFP) (*A*) or the cDNA for DrVSP (*B*). The pipette solution contained 0.05 mM EGTA and pH_i was maintained at 7.2. Cells were held at −60 mV and currents continuously recorded while a depolarization pulse to 100 mV for 1 s to activate DrVSP, followed by −60 mV for 0.5 s and then a voltage ramp from +100 to −100 mV for 0.5 s (inset in *A*), were applied every 5 s. Whole-cell currents were evoked by EA (100 nM). *A* and *B*, representative current traces. Currents before (I_0) and after (*I*) the depolarization pulse during the episode pointed by the red cones are expanded to the right. *C* and *D*, summary (means ± SD and data points of individual cells) of peak current density at −60 mV (*C*) and I/I_0 ratio (*D*), showing no significant effect of PIP_2 depletion by DrVSP. *E–G*, intracellular Ca^{2+} dependence of TRPC4 activation by EA. Cells stably co-expressing μOR and TRPC4β were used. Pipette solutions contained either 0.05 or 5 mM EGTA with no Ca^{2+} added (*E*, *F*) or 5 mM BAPTA with Ca^{2+} added to clamp $[Ca^{2+}]_i$ to 10, 100, 400, 1000 or 3000 nM (*G*). pH_i was 7.2 for all pipette solutions. The bath solution contained 2 mM Ca^{2+}. Whole-cell TRPC4 currents were elicited by 100 nM EA. The voltage protocol followed that of Fig. 1. *E*, representative current traces for internal solutions that contained 0.05 mM (upper panel) and 5 mM (lower panel) EGTA. *F*, summary (means ± SD and data points of individual cells) of peak current

density at −60 mV for conditions in *E*. $^{**}p < 0.01$ by unpaired *t* test. *G*, peak current density at +100 and −100 mV evoked by EA with $[Ca^{2+}]_i$ clamped at different levels. Data are means ± SD for the numbers of cells indicated in parentheses. Continuous lines are fits to a biphasic Hill equation, which yielded EC_{50} values of 298 nM ($n_H = 2.98$) at +100 mV and 255 nM ($n_H = 3.24$) at −100 mV for Ca^{2+}-dependent potentiation and IC_{50} values of 2.1 μM ($n_H = -1.73$) at +100 mV and 1.9 μM ($n_H = -1.26$) for Ca^{2+} inhibition. *H*, lowering pH_i suppressed EA-evoked TRPC4 currents. Cells stably co-expressing μOR and TRPC4β were used. The pipette solution contained 5 mM NaAc and 400 nM free $[Ca^{2+}]_i$ clamped with 5 mM BAPTA with pH_i of 7.4. The voltage protocol and data display followed that of Fig. 1. To prevent desensitization, a Ca^{2+}-free bath solution (with 1 mM EGTA) was applied before the addition of 10 nM EA. After the current had stabilized, pH_i was changed to 6.5 through bath application of 39.5 mM NaAc solution in the continued presence of EA in the Ca^{2+}-free condition. Note the decrease in current amplitude. *I*, summary of current density before and after switching to pH_i 6.5. Data points of individual cells are connected. $^{**}p < 0.01$ by paired *t* test.

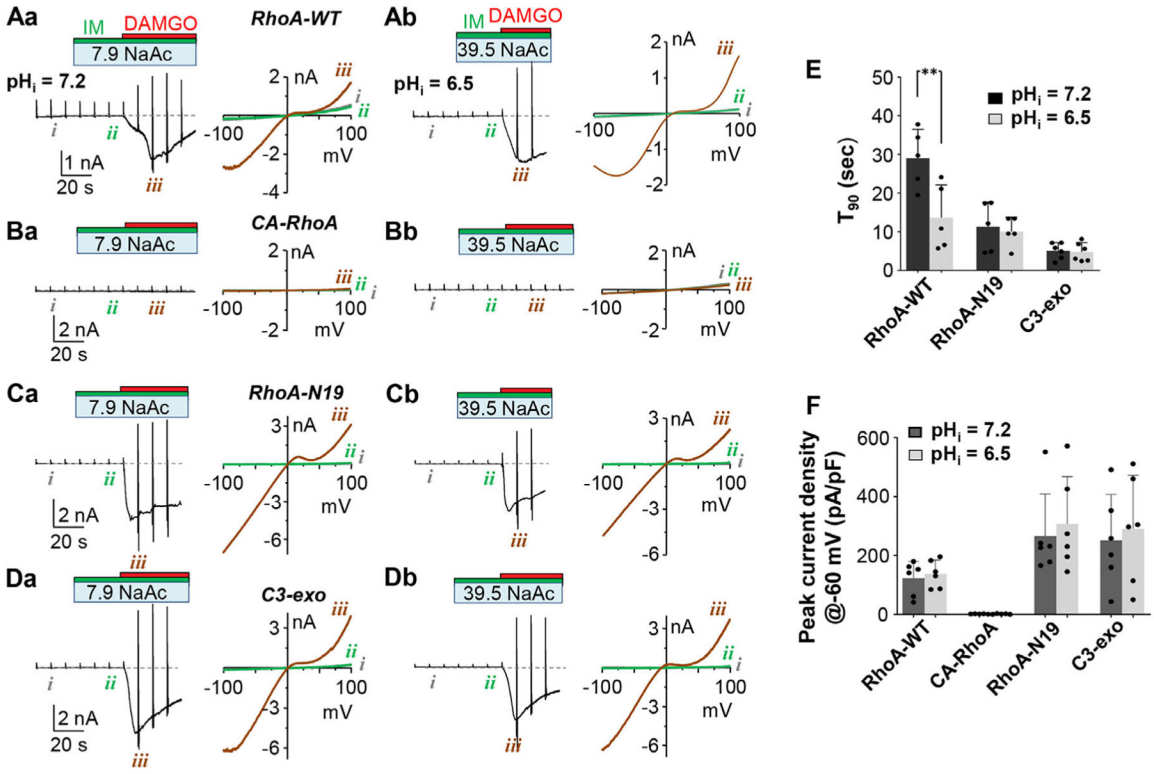

Figure 5. RhoA suppresses the facilitatory action of intracellular protons on $G_{i/o}$-mediated TRPC4 activation

A–D, representative time courses of currents at −60 mV (left panels) and *I–V* curves (right panels) of cells stably co-expressing μOR with TRPC4β and transiently transfected with the cDNA for wild type RhoA (RhoA-WT, *A*), constitutively active mutant of RhoA (CA-RhoA, *B*), dominant-negative mutant of RhoA (RhoA-N19, *C*) and the RhoA inhibitor C3 exoenzyme (C3-exo, *D*). The pipette solution contained 0.05 mM EGTA and 5 mM NaAc, pH 7.4. To clamp pH_i to 7.2 (*Aa–Da*) and 6.5 (*Ab–Db*), NaAc was bath applied to 7.9 and 39.5 mM, respectively. IM (1 μM) was applied at the same time as NaAc and DAMGO applied about 30 s later, as indicated, to increase $[Ca^{2+}]_i$ and stimulate $G_{i/o}$ via μOR, respectively. *E* and *F*, summary of T_{90} (*E*) and peak current density at −60 mV (*F*) for the conditions indicated. Voltage protocols and display conventions follow that of Fig. 1. $^{**}p < 0.01$, by ANOVA with Tukey's multiple comparisons test. Note, CA-RhoA suppressed $G_{i/o}$-mediated TRPC4 activation at both pH_i 7.2 and pH_i 6.5; inactivating RhoA with either RhoA-N19 or C3-exo, which disinhibits PLCδ1, abolished the need for low pH_i to accelerate $G_{i/o}$-mediated TRPC4 activation.

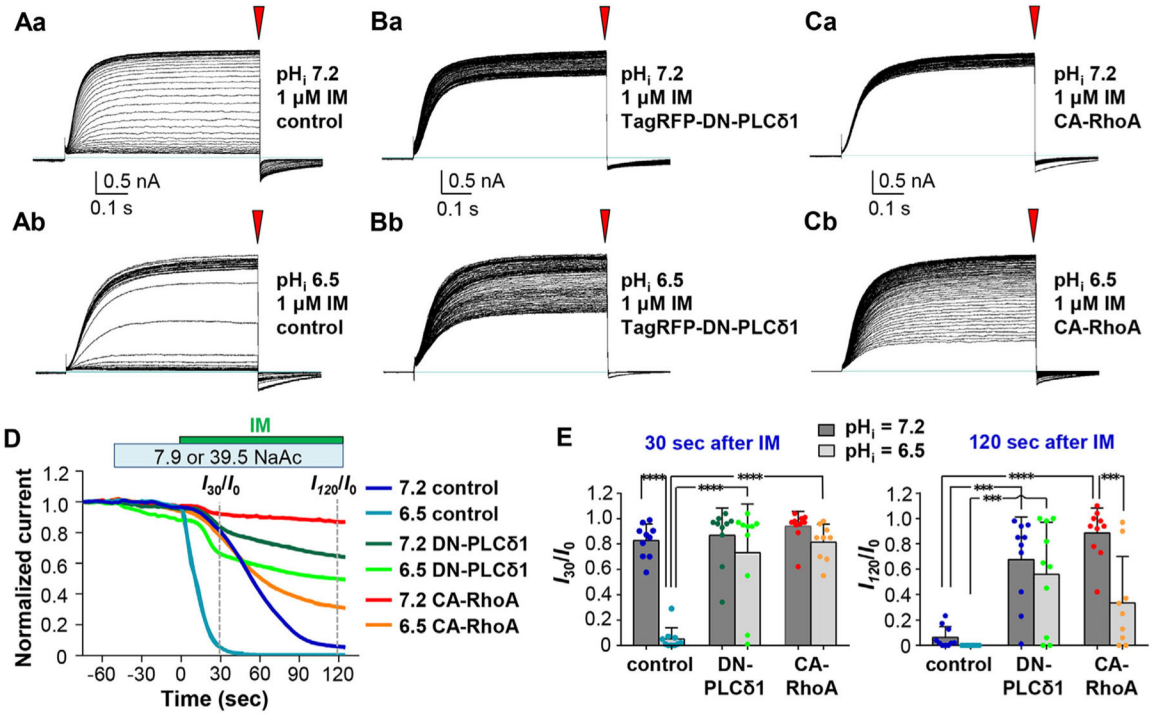

Figure 6. Intracellular acidification facilitates Ca^{2+}-dependent activation of PLCδ1 in the absence of TRPC4

HEK293 cells stably expressing μOR were transiently cotransfected with the cDNA constructs for KCNQ2, KCNQ3-CFP, in the absence (*A*) or presence of the cDNA for a dominant-negative mutant of PLCδ1 (TagRFP-DN-PLCδ1, *B*) or the cDNA for a constitutively active mutant of RhoA (CA-RhoA, *C*). K^+-based pipette solution contained 0.05 mM EGTA and 5 mM NaAc with pH_i of 7.4, while bath solutions had 5 mM K^+ and 2 mM Ca^{2+}, pH 7.4, and other ingredients as described in Methods. Whole-cell currents of KCNQ2/3 were elicited by repeated depolarization steps from the holding potential of −60 mV to 0 mV for 0.6 s at 0.4 Hz. Cells were recorded in the normal bath for 25 s to establish the baseline current. The bath was then changed to the one containing 7.9 or 39.5 mM NaAc, pH 7.4, to drop pH_i to 7.2 (*Aa–Ca*) or 6.5 (*Ab–Cb*), respectively, for 50 s before 1 μM IM was added to elevate $[Ca^{2+}]_i$, which caused a time-dependent decrease in KCNQ2/3 current due to reduction of PIP_2 levels by PLC. *A–C*, representative current traces. Note the rapid current decline, as indicated by the small number of intermediate-sized traces, and the complete current inhibition in *Ab*. Currents are displayed without leak subtraction. Red arrows indicate the time point when steady-state currents were used for analysis in *D* and *E*. *D*, time courses of steady-state KCNQ2/3 currents at 0 mV under the different conditions indicated. Currents without leak subtraction were normalized to that at the beginning of the recording. Data are averages from 9–10 cells for each condition. Grey dashed lines indicate 30 and 120 s after IM addition, from which I_{30}/I_0 and I_{120}/I_0 ratios of individual cells were extracted for statistical analysis shown in *E*. *E*, means ± SD and data points of individual cells. ***$p < 0.001$, ****$p < 0.0001$ by ANOVA with Tukey's multiple comparisons test.

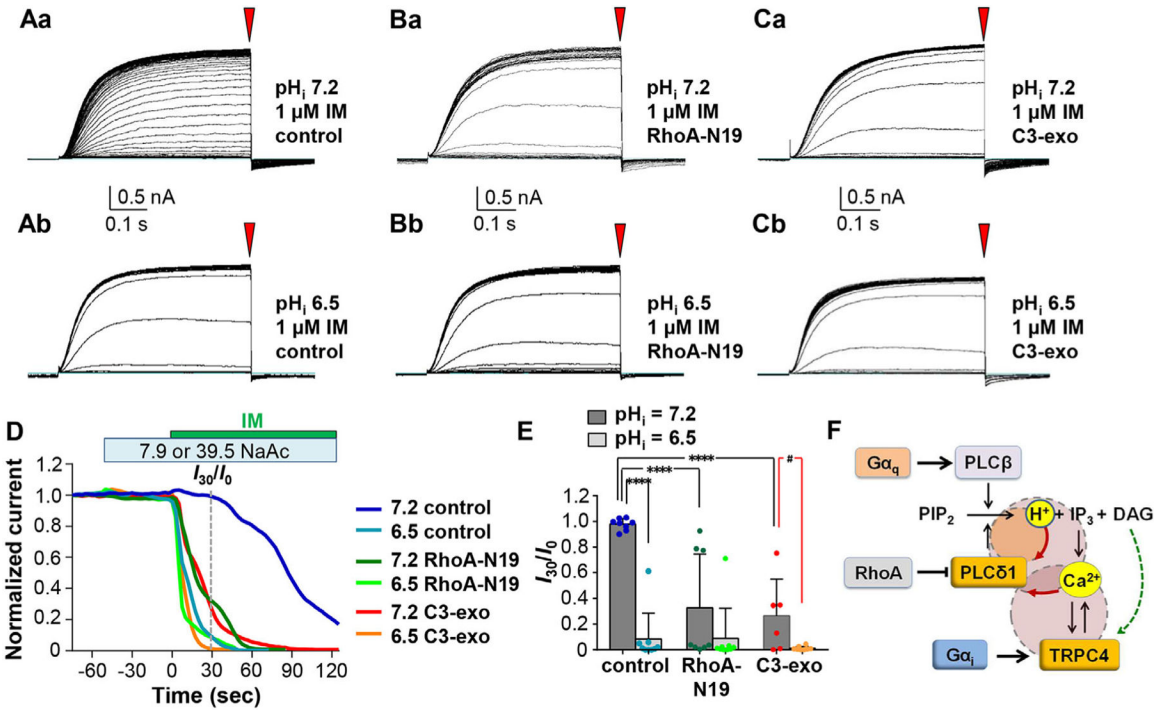

Figure 7. RhoA inhibition facilitates Ca^{2+}-dependent activation of PLCδ1 in the absence of TRPC4

HEK293 cells stably expressing μOR were transiently cotransfected with the cDNA constructs for KCNQ2, KCNQ3-CFP, in the absence (*A*) or presence of the cDNA for a dominant-negative mutant of RhoA (RhoA-N19, *B*) or RhoA inhibitor, C3 exoenzyme (C3-exo, *C*). Whole-cell recordings followed that of Fig. 6. *A–C*, representative current traces. Note the rapid current decline in cells that co-expressed RhoA-N19 or C3-exo at both pH_i 7.2 and pH_i 6.5 and the complete current inhibition. Currents are displayed without leak subtraction. Red arrows indicate the time point when steady-state currents were used for analysis in *D* and *E*. *D*, time courses of steady-state KCNQ2/3 currents at 0 mV under different conditions indicated. Currents without leak subtraction were normalized to that at the beginning of the recording. Data are averages from 6–9 cells for each condition. Grey dashed line indicates 30 s after IM addition, from which I_{30}/I_0 ratios of individual cells were extracted for the statistical analysis shown in *E*. *E*, means ± SD and data points of individual cells. ***$p < 0.001$, ****$p < 0.0001$ by ANOVA with Tukey's multiple comparisons test. $^{\#}p < 0.05$ by unpaired *t* test. *F*, schematic diagram of TRPC4 activation coregulated by $G_{q/11}$ and $G_{i/o}$ signalling, and the critical role of protons through PLCδ1. Positive feedback loops evolving around intracellular H^+ and Ca^{2+} are shown as circles surrounded by the dashed lines. While protons may only propagate alongside PLCδ1, which acts as both the sensor and the producer of the H^+ signal, Ca^{2+} is sensed and produced by both PLCδ1 (through IP_3 and IP_3 receptors) and TRPC4. These propagating activities make the activation of TRPC4 all-or-none. Activation of $G_{q/11}$-PLCβ (or RTK-PLCγ, not shown) or inactivation of RhoA helps enter the self-propagating mode, as will the increases in intracellular H^+ and Ca^{2+} levels.